Structural Determination of Lysophospholipid Regioisomers by Electrospray Ionization Tandem Mass Spectrometry†

Xianlin Han and Richard W. Gross*

Contribution from the Division of Bioorganic Chemistry and Molecular Pharmacology, Departments of Medicine, Chemistry, and Molecular Biology & Pharmacology, Washington University School of Medicine, St. Louis, Missouri 63110

Received July 14, 1995[⊗]

Abstract: The facile structural determination of lysophospholipid regioisomers represents a long-standing problem in phospholipid chemistry. Herein we report that positive-ion electrospray ionization (ESI) tandem mass spectrometry of sodiated lysophospholipid regioisomers results in the presence of multiple diagnostic pairs of product ions which allows the rapid and direct discrimination between *sn*-1-acyl- and *sn*-2-acyllysophospholipid regioisomers. For example, after ESI in the positive-ion mode and subsequent collision-induced dissociation, over a 30-fold difference in the peak intensity ratio of product ions at *m*/*z* 104 and 147 was manifest with sodiated *sn*-1-acyllysophosphatidylcholine in comparison to *sn*-2-acyllysophosphatidylcholine. The observed differences in precursor ion dissociation rates reflect both the kinetically favored formation of a 5-membered phosphodiester (compared to the corresponding 6-membered phosphodiester) and the accelerated rate of an activated vs a nonactivated rearrangement. The structure of individual molecular species and classes of lysophospholipids was substantiated after ESI in the negative-ion mode by tandem mass spectrometry which facilitated identification of lysophospholipid aliphatic constituents and polar head groups. Thus, by exploiting the remarkable sensitivity of electrospray ionization in conjunction with the combined utilization of tandem mass spectrometry in both the positive- and negative-ion modes, structural determination of the specific regioisomer, individual molecular species, and class of lysophospholipids is possible from picomole amounts of material.

Introduction

The discrimination between individual regioisomers of lysophospholipids (e.g., 1-acyl-2-hydroxy-*sn*-glycero-3-phosphocholine vs 1-hydroxy-2-acyl-*sn*-glycero-3-phosphocholine) has represented a formidable obstacle in membrane chemistry. Due to its mechanistic implications (e.g., identification of the class of phospholipases activated during cellular stimulation and their phospholipid substrates) and synthetic importance,[1−13] the direct structural determination of lysophospholipid regioisomers from organic extracts of biologic tissues, where diminutive amounts of materials are available, has been a long-standing goal of phospholipid chemistry.[14−19] However, this goal has not been realized, in part due to the rapid intrapreparative isomerization of lysophospholipid regioisomers catalyzed by silica-based stationary phases leading to α-hydroxy acyl migration.[4,19−22] Furthermore, although NMR methods have successfully been utilized in the structural determination of lysophospholipid regioisomers,[16,19] the amounts of mass typically required for NMR analyses preclude its routine use in analyses of lysolipid isomers in biologic samples.

Negative-ion fast atom bombardment tandem mass spectrometry has been successfully employed in the determination of the acyl chain regioisomers in asymmetrical diacyl glycerophospholipids through comparisons of the intensity ratio of *sn*-1- and *sn*-2-carboxylate ions derived from the cleavage of the acyl constituents after collisional activation.[23−25] However, since only one acyl chain is present in lysophospholipids, similar comparisons are not germane to the discrimination between lysophospholipid regioisomers. Recently, we identified the

* Author to whom correspondence should be addressed: Richard W. Gross, M.D., Ph.D., Division of Bioorganic Chemistry and Molecular Pharmacology, Washington University School of Medicine, 660 South Euclid, Box 8020, St. Louis, MO 63110. Telephone number: 314-362-2690. FAX number: 314-362-1402.

[⊗] Abstract published in *Advance ACS Abstracts,* December 15, 1995.

(1) Dennis, E. A. *J. Biol. Chem.* **1994**, *269*, 13057−13060.
(2) Dennis, E. A.; Rhee, S. G.; Billah, M. M.; Hannun, Y. A. *FASEB J.* **1991**, *5*, 2068−2077.
(3) Yu, L.; Dennis, E. D. *Proc. Natl. Acad. Sci. U.S.A.* **1991**, *88*, 9325−9329.
(4) Gupta, C. M.; Radhakrishnan, R.; Khorana, H. G. *Proc. Natl. Acad. Sci. U.S.A.* **1977**, *74*, 4315−4319.
(5) Warner, T. G.; Benson, A. A. *J. Lipid Res.* **1977**, *18*, 548−552.
(6) Homma, H.; Nishijima, M.; Kobayashi, T.; Okuyama, H.; Nojima, S. *Biochim. Biophys. Acta* **1981**, *663*, 1−13.
(7) Han, X.; Zupan, L. A.; Hazen, S. L.; Gross, R. W. *Anal. Biochem.* **1992**, *200*, 119−124.
(8) Kumar, R.; Weintraub, S. T.; McManus, L. M.; Pinckard, R. N.; Hanahan, D. J. *J. Lipid Res.* **1984**, *25*, 198−208.
(9) Weltzien, H. U. *Biochim. Biophys. Acta* **1979**, *559*, 259−287.
(10) Man, R. Y. K.; Kinnaird, A. A. A.; Bihler, L.; Choy, P. C. *Lipids* **1990**, *25*, 450−454.
(11) Liu, E.; Goldhaber, J. I.; Weiss, J. N. *J. Clin. Invest.* **1991**, 1819−1832.
(12) Quinn, M. T.; Konodratenko, N.; Parthasarathy, S. *Biochim. Biophys. Acta* **1991**, *1082*, 293−302.
(13) Vesterquist, O.; Sargent, C. A.; Taylor, S. C.; Newburger, J.; Tymiak, A. A.; Grover, G. J.; Ogletree, M. L. *Anal. Biochem.* **1992**, *204*, 72−78.
(14) Slotboom, A. J.; de Haas, G. H.; van Deenen, L. L. M. *Chem. Phy. Lipids* **1967**, *1*, 317−336.
(15) Satouchi, K.; Saito, K. *Biomed. Mass Spectrom.* **1977**, *4*, 107−112.
(16) Schmidt, C. F.; Barenholz, Y.; Huang, C.; Thompson, T. E. *Biochemistry* **1977**, *16*, 3948−3954.
(17) Sugatani, J.; Okumura, T.; Saito, K. *Biochim. Biophys. Acta* **1980**, *620*, 372−386.
(18) Matsuzawa, Y.; Hostetler, K. Y. *J. Biol. Chem.* **1980**, *255*, 646−652.
(19) Plückthun, A.; Dennis, E. A. *Biochemistry* **1982**, *21*, 1743−1750.
(20) Pavlova, L. V.; Rachinskii, F. Y. *Russ. Chem. Rev. (Engl. Transl.)* **1968**, *37*, 587−602.
(21) Eibl, H.; Lands, W. E. W. *Biochemistry* **1970**, *9*, 423−428.
(22) Creer, M. H.; Gross, R. W. *Lipids* **1985**, *20*, 922−928.
(23) Jensen, N. J.; Tomer, K. B.; Gross, M. L. *Lipids* **1986**, *21*, 580−588.
(24) Kayganich, K.; Murphy, R. C. *J. Am. Soc. Mass Spectrom.* **1991**, *2*, 45−54.
(25) Huang, Z.-H.; Gage, D. A.; Sweeley, C. C. *J. Am. Soc. Mass Spectrom.* **1992**, *3*, 71−78.

0002-7863/96/1518-0451$12.00/0

utility of electrospray ionization mass spectrometry for the analysis of individual phospholipid molecular species from subpicomole amounts of synthetic and naturally occurring membrane phospholipids[26] and demonstrated that collision-induced dissociation of precursor ions generated from electrospray ionization often resulted in novel product-ion patterns.[27] Herein, we exploit the remarkable sensitivity of positive-ion ESI tandem mass spectrometry for the direct structural determination of picomole amounts of lysophospholipid regioisomers through comparisons of the relative abundance of critical pairs of diagnostic ions and identify the likely pathways responsible for the differences in their relative abundance after collision-induced dissociation.

Experimental Section

Materials. All commercially available phospholipids were obtained from Avanti Polar Lipids, Inc. (Alabaster, AL) except polyunsaturated *sn*-1-lysophosphatidylcholines which were purchased from Serdary Research Labs, Inc. (London, Ontario, Canada). All purchased *sn*-1-monoacyllysophospholipids were further purified by reverse phase HPLC as previously described[22] prior to the ESI mass spectroscopic analyses. All *sn*-2-monoacyllysophospholipids were freshly prepared by the method of Slotboom et al.[14] utilizing *Rhizopus arrhizus* lipase (phospholipase A_1, Sigma), followed by reverse phase HPLC purification.[22] Lysoplasmenylcholines and lysoplasmenylethanolamines were prepared as previously described.[7] The mass of phospholipids employed in this study was quantitated either by direct ESI-MS analysis[26] and/or capillary gas chromatography after acid methanolysis.[28]

Electrospray Ionization Tandem Mass Spectrometry of Lysophospholipid Regioisomers. ESI tandem mass spectrometry was performed using a triple-quadrupole tandem mass spectrometer (Finnigan MAT TSQ 700, San Jose, CA) equipped with an ESI interface (Analytica of Branford, Branford, CT) as previously described in detail.[26] Briefly, molecular ions of lysophospholipids were voltalized by ESI, selected after passage through the first quadrupole with a mass-selected window of less than 2 mass units, and subsequently collisionally dissociated in the second quadruple using argon gas. The resultant product ions were subsequently analyzed in the third quadruple. During this study, collision energies of approximately 20 eV (with respect to the laboratory reference) were employed (except as indicated) and collision gas pressures of approximately 3 mTorr were utilized. All product-ion spectra were acquired using a signal-averaging protocol in the profile mode with a scan rate of 200 amu/s. Typically, a 5-min period of signal averaging was used for each tandem mass spectrum, and the mass of all ions was rounded to the nearest integer. All samples (1 pmol/μL) were dissolved in 1:2 chloroform/methanol and infused directly into the ESI chamber using a syringe pump (Harvard Apparatus, South Natick, MA) at a flow rate of 1.5 μL/min for 5 min. Sodiated lysophospholipid (the only ion displayed in the positive-ion mass spectrum (Figure 1)) was the mass-selected precursor ion utilized for positive-ion ESI tandem mass spectrometry. Deprotonated ions of ethanolamine lysophospholipids (the only ion generated from negative-ion ESI) were mass-selected and utilized for negative-ion ESI tandem mass spectrometry of ethanolamine lysophospholipids. During the performance of the negative-ion ESI tandem mass spectrometry of choline lysophospholipids, chloride ion (from NaCl) was added to the sample solution prior to infusion into the ESI chamber and the chlorine adduct of choline lysophospholipid was the precursor ion employed.

Results and Discussion

Positive-Ion ESI Tandem Mass Spectrometry of Choline Lysophospholipid Regioisomers. The utility of ESI tandem mass spectrometry for discrimination between lysophospholipid regioismers was first appreciated by comparison of the positive-ion ESI tandem mass spectra of *sn*-1- and *sn*-2-lysophosphatidylcholine regioisomers (i.e., 1-hexadecanoyl-2-hydroxy-*sn*-glycero-3-phosphocholine and 1-hydroxy-2-hexadecanoyl-*sn*-glycero-3-phosphocholine). Collision-induced dissociation of sodiated 1-hexadecanoyl-2-hydroxy-*sn*-glycero-3-phosphocholine after ESI in the positive-ion mode resulted in the appearance of multiple informative product ions (Figure 2A). The most abundant product ion, *m*/*z* 459 (i.e., $[M + Na - 59]^+$), corresponds to the neutral loss of trimethylamine. Less abundant product ions were present at *m*/*z* 415 (i.e., $[M + Na - 103]^+$), 313 (i.e., $[M + Na - 205]^+$), 147 (likely the sodiated 5-membered cyclophosphane), and 104 (likely choline) (Figure 2A).

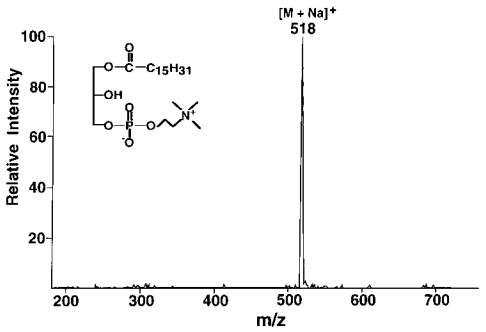

Figure 1. Positive-ion electrospray ionization mass spectrum of lysophosphatidylcholine. A positive-ion ESI mass spectrum of 1-hexadecanoyl-2-hydroxy-*sn*-glycero-3-phosphocholine (1 pmol/μL) obtained during a 1-min infusion at a flow rate of 1.5 μL/min under the conditions given in the Experimental Section shows a single molecular ion at *m*/*z* 518 ($[M + Na]^+$). No fragments of the molecular ion were present in the spectrum at the extraction voltage employed (i.e., 90 V).

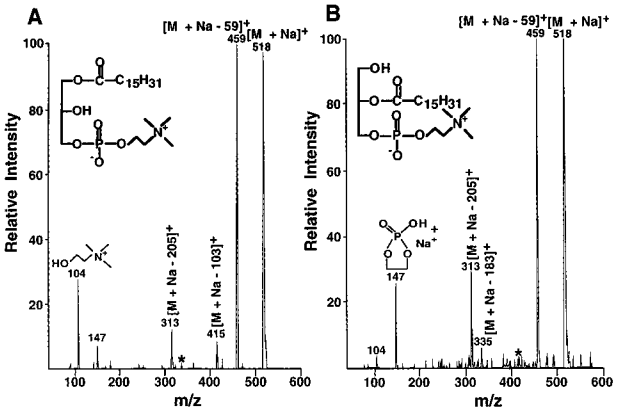

Figure 2. Positive-ion electrospray ionization tandem mass spectra of choline lysophospholipid regioisomers. Positive-ion ESI tandem mass spectra of sodiated 1-hexadecanoyl-2-hydroxy-*sn*-glycero-3-phosphocholine (A) and sodiated 1-hydroxy-2-hexadecanoyl-*sn*-glycero-3-phosphocholine (B) were obtained as described in the Experimental Section. Samples (1 pmol/μL) were dissolved in 1:2 chloroform/methanol and infused directly into the ESI chamber using a syringe pump at a flow rate of 1.5 μL/min for 5 min. The stars indicate the product ions at *m*/*z* 335 in panel A and *m*/*z* 415 in panel B present in very low abundance.

Collision-induced dissociation of sodiated 1-hydroxy-2-hexadecanoyl-*sn*-glycero-3-phosphocholine after ESI in the positive-ion mode resulted in the appearance of multiple prominent product ions including ions at *m*/*z* 459, 335, 313, 147, and 104 (Figure 2B) which were present in the positive-ion ESI tandem mass spectrum of sodiated 1-hexadecanoyl-2-hydroxy-*sn*-glycero-3-phosphocholine (Figure 2A). However, the ratios of the peak intensities of specific product-ion pairs from each lysophosphatidylcholine regioisomer were dramatically different. For example, the peak intensity ratio of product ions at *m*/*z* 104 and 147 differed by over 30-fold in individual

(26) Han, X.; Gross, R. W. *Proc. Natl. Acad. Sci. U.S.A.* **1994**, *91*, 10635−10639.
(27) Han, X.; Gross, R. W. *J. Am. Soc. Mass Spectrom.* **1995**, *6*, 1202−1210.
(28) Fink, K. L.; Gross, R. W. *Circ. Res.* **1984**, *55*, 585−594.

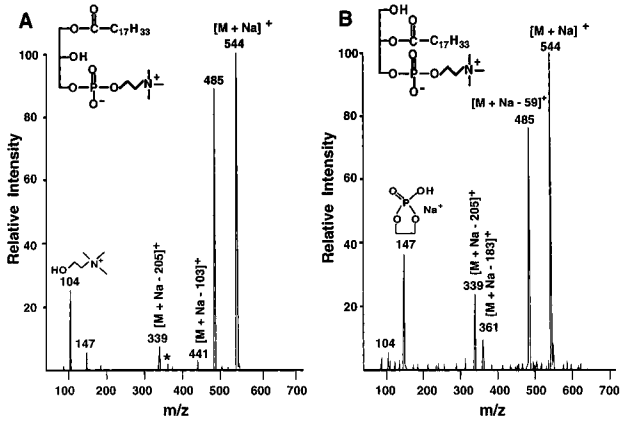

Figure 3. Positive-ion electrospray ionization tandem mass spectra of choline lysophospholipid regioisomers. Positive-ion ESI tandem mass spectra of sodiated 1-octadec-9′-enoyl-2-hydroxy-*sn*-glycero-3-phosphocholine (A) and sodiated 1-hydroxy-2-octadec-9′-enoyl-*sn*-glycero-3-phosphocholine (B) were obtained as described in the Experimental Section. Samples (1 pmol/μL) were dissolved in 1:2 chloroform/methanol and infused directly into the ESI chamber using a syringe pump at a flow rate of 1.5 μL/min for 5 min. The star indicates the product ion at *m*/*z* 361 in panel A present in very low abundance.

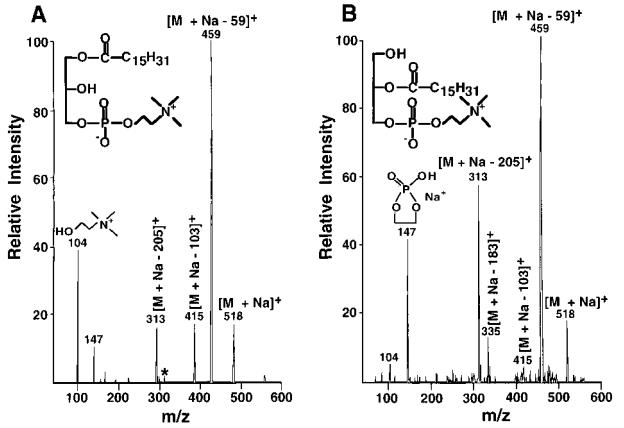

Figure 4. Positive-ion electrospray ionization tandem mass spectra of choline lysophospholipid regioisomers acquired at a higher collision energy. Positive-ion ESI tandem mass spectra of sodiated 1-hexadecanoyl-2-hydroxy-*sn*-glycero-3-phosphocholine (A) and sodiated 1-hydroxy-2-hexadecanoyl-*sn*-glycero-3-phosphocholine (B) were obtained as described in the Experimental Section utilizing an offset voltage of 40 eV (note the collision energy utilized for spectra in Figure 2 was 20 eV). All other conditions are identical to those as described in Figure 2.

regioisomers (i.e., 4:1 after dissociation of sodiated 1-hexadecanoyl-2-hydroxy-*sn*-glycero-3-phosphocholine and 1:8 after dissociation of sodiated 1-hydroxy-2-hexadecanoyl-*sn*-glycerol-3-phosphocholine) (Figure 2). Furthermore, the product ion at *m*/*z* 313 (i.e. $[M + Na - 205]^+$ ion) present after dissociation of the sodiated *sn*-1 isomer is less abundant than that from the sodiated *sn*-2 isomer (Figure 2). Finally, the *m*/*z* 415 ion (i.e., $[M + Na - 103]^+$) is nearly absent in the ESI tandem mass spectrum of the *sn*-2 isomer (Figure 2B) but represents a major product ion after collision-induced dissociation of the sodiated *sn*-1-acyllysophosphatidylcholine (Figure 2A).

To determine if the observed differences in the relative peak intensities of product ions obtained after collision-induced dissociation of sodiated lysophosphatidylcholines generated by ESI in the positive-ion mode can be routinely utilized for the discrimination of lysophosphatidylcholine regioisomers, *sn*-1 and *sn*-2 isomers differing in chain lengths (between 14 and 20 carbons) and degree of unsaturation ($n = 0-4$) were examined. The product-ion patterns of multiple different regioisomers of each molecular species were nearly identical to those obtained for 1- or 2-hexadecanoyl-*sn*-glycero-3-phosphocholine regioisomers. For example, positive-ion ESI tandem mass spectra of sodiated 1-octadec-9′-enoyl-2-hydroxy-*sn*-glycero-3-phosphocholine (Figure 3A)) contained diagnostic pairs of product ions at *m*/*z* 104 (corresponding to choline) and 147 (corresponding to a sodiated 5-membered cyclophosphane) in approximately a 4:1 ratio while tandem mass spectra of sodiated 1-hydroxy-2-octadec-9′-enoyl-*sn*-glycero-3-phosphocholine contained these ions in a 1:8 ratio (Figure 3B).

To clarify the effects of differences in collision energies on the ion dissociation patterns of individual regioisomers, additional positive-ion ESI tandem mass spectrometric analyses of sodiated lysophosphatidylcholine regioisomers were performed. Increasing the dc offset voltage increased product-ion peak intensities, but the relative ratios of product ions and therefore the relative peak intensities of the diagnostic product ion pairs (e.g., *m*/*z* 104 and 147) were not altered. For example, the positive-ion ESI tandem mass spectra of sodiated 1-hexadecanoyl-2-hydroxy-*sn*-glycero-3-phosphocholine and sodiated 1-hydroxy-2-hexadecanoyl-*sn*-glycero-3-phosphocholine acquired at a dc offset voltage of 40 eV were nearly identical to

Scheme 1. Proposed Collision-Induced Dissociation Pathways of Sodiated 1-Acyl-2-hydroxy-*sn*-glycero-3-phosphocholines

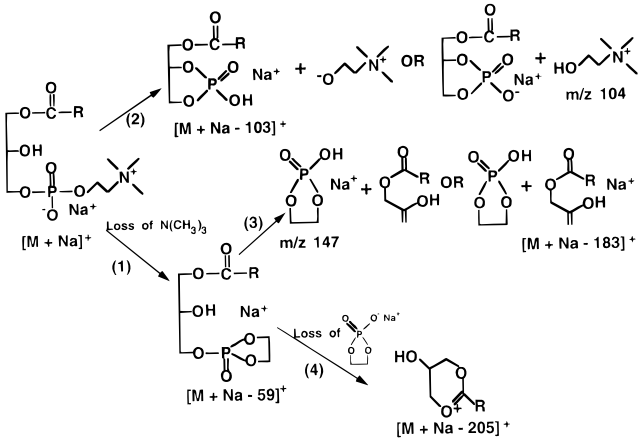

the spectra taken at 20 eV (compare Figure 4 to Figure 2), demonstrating that the ratio of the diagnostic pair of product ions at *m*/*z* 104 and 147 is largely independent of routinely employed dc offset voltages.

Proposed Dissociation Pathways of Sodiated Choline Lysophospholipid Regioisomers. The observed product-ion patterns likely arise from the collision-induced dissociation of sodiated 1-acyl- and 2-acyllysophosphatidylcholines through pathways illustrated in Schemes 1 and 2, respectively. The critical features of these pathways include (1) the neutral loss of trimethylamine (pathway 1) resulting in the generation of sodiated 1-acyl- or 2-acyl-*sn*-glycero-3-cyclo(1′,2′-ethylene glycol)phosphodiester (i.e., $[M + Na - 59]^+$); (2) either the neutral loss of choline resulting in the generation of sodiated monoacyl glycerophosphodiester (i.e., $[M + Na - 103]^+$) or the neutral loss of monoacyl glycerophosphodiester resulting in the generation of choline (*m*/*z* 104) through the formation of a cyclic phosphodiester (pathway 2); (3) a rearrangement resulting in the generation of either a sodiated 5-membered cyclophosphane (*m*/*z* 147) or a sodiated monoacyl glycerol derivative (i.e., $[M + Na - 183]^+$) from $[M + Na - 59]^+$ (pathway 3); and (4) the neutral loss of sodium cyclophosphate resulting in the generation of a monoacyl glycerol derivative cation (i.e., [M +

Scheme 2. Proposed Collision-Induced Dissociation Pathways of Sodiated 1-Hydroxy-2-acyl-*sn*-glycero-3-phosphocholines

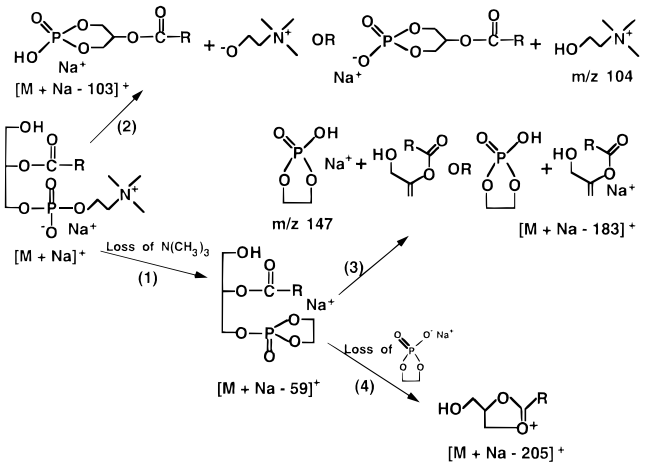

$Na - 205]^+$) (pathway 4). Since these pathways emanate from a common molecular ion, the relative abundance of product ions is directly related to the relative enthalpic and entropic changes inherent in each pathway. Clearly, pathway 1 is favored for both regioisomers since the product ion $[M + Na - 59]^+$ is always the most abundant product ion from choline-containing phospholipids. The predominant product ion of sodiated 1-acyl-2-hydroxy-*sn*-glycero-3-phosphocholine corresponds to the favored 5-membered phosphodiester (pathway 2 in Scheme 1) and leads to the formation of choline (*m*/*z* 104) (Figures 2A and 3A) while the 6-membered phosphodiester (pathway 2 in Scheme 2) is required for the generation of choline from sodiated 1-hydroxy-2-acyl-*sn*-glycero-3-phosphocholine. Similarly, the product ion $[M + Na - 205]^+$ from sodiated 1-hydroxy-2-acyl-*sn*-glycero-3-phosphocholine dissociation results from the formation of a 5-membered ion (pathway 4 in Scheme 2) while the corresponding 6-membered analog formed from sodiated 1-acyl-2-hydroxy-*sn*-glycerol-3-phosphocholine (pathway 4 in Scheme 1) is present in lower relative abundance (e.g., compare Figure 2A to 2B). Dissociation pathway 3 is effected through either an activated rearrangement in the case of sodiated 1-hydroxy-2-acyl-*sn*-glycero-3-phosphocholine (activated by the electron-withdrawing properties of the ester group, pathway 3 in Scheme 2) or a nonactivated rearrangement in the case of sodiated 1-acyl-2-hydroxy-*sn*-glycero-3-phosphocholine (pathway 3 in Scheme 1). Further, dissociation pathway 3 in the case of sodiated 1-acyl-2-hydroxy-*sn*-glycero-3-phosphocholine (Scheme 1) requires the formation of a vinyl alcohol which is less stable than the corresponding formation of a vinyl ester from sodiated 1-hydroxy-2-acyl-*sn*-glycero-3-phosphocholine (Scheme 2). Accordingly, product ions at *m*/*z* 147 and $[M + Na - 183]^+$ are more abundant after collision-induced dissociation of sodiated 1-hydroxy-2-acyl-*sn*-glycero-3-phosphocholine (Figures 2B and 3B) in comparison to those generated from sodiated 1-acyl-2-hydroxy-*sn*-glycero-3-phosphocholine (Figures 2A and 3A).

To support the collision-induced dissociation pathways of sodiated choline lysophospholipid regioisomers proposed herein, additional positive-ion ESI tandem mass spectroscopic analyses were performed utilizing lysophospholipid subclasses containing different covalent linkages to the *sn*-1 carbon (e.g., 1-*O*-*(Z)*-alk-1′-enyl-2-hydroxy-*sn*-glycero-3-phosphocholines (lysoplasmenylcholine) and 1-*O*-alkyl-2-hydroxy-*sn*-glycero-3-phosphocholines (lysoplasmanylcholine). The positive-ion ESI tandem mass spectra of sodiated lysoplasmenylcholine (Figure 5A) and sodiated lysoplasmanylcholine (Figure 5B) were nearly identical to those of the corresponding sodiated 1-acyl-2-hydroxy-*sn*-glycero-3-phosphocholine in that a relative ratio of 4:1 for product ions at *m*/*z* 104 and 147 was present. As anticipated, the product ion $[M + Na - 205]^+$ was not present since the ester group is absent in lysoplasmenylcholine and lysoplasmanylcholine, and thus pathway 4 in Scheme 1 is untenable. For 1-*O*-alkyl-2-acetyl-*sn*-glycero-3-phosphocholines (PAF) where an *sn*-2-acyl group is present in the absence of either *sn*-1- or *sn*-2-hydroxys, pathway 2 in Schemes 1 and 2 is not possible and thus product ions at $[M + Na - 103]^+$ and choline (*m*/*z* 104) are not present in the positive-ion ESI tandem mass spectra of sodiated PAF (Figure 5C, compared with Figures 2, 3, and 5A,B).

Positive-Ion ESI Tandem Mass Spectrometry of Ethanolamine Lysophospholipid Regioisomers. The utility of ESI tandem mass spectrometry for discrimination between lysophospholipid regioisomers containing ethanolamine polar head groups was demonstrated by comparison of positive-ion ESI tandem mass spectra of lysophosphatidylethanolamine regioisomers. Corresponding pairs of *sn*-1- and *sn*-2-ethanolamine lysophospholipid regioisomers (i.e., C14:0, C16:0, C18:1) were separated by reverse phase HPLC as described in the Experimental Section and analyzed by positive-ion ESI tandem mass spectrometry. The product ion patterns were nearly identical for molecular species containing different acyl chains, but were dramatically different for regioisomers of each molecular species. For example, positive-ion ESI tandem mass spectra of sodiated 1-octadec-9′-enoyl-2-hydroxy-*sn*-glycero-3-phosphoethanolamine (*sn*-1-acyllysophosphatidylethanolamine) and sodiated 1-hydroxy-2-octadec-9′-enoyl-*sn*-glycero-3-phosphoethanolamine (*sn*-2-acyllysophosphatidylethanolamine) after ESI in the positive-ion mode were remarkable for ions at *m*/*z* 459, 441, 361, 339, 164, and 121 (Figure 6). The most abundant product ion *m*/*z* 459 ($[M + Na - 43]^+$) corresponds to sodiated *sn*-1- or *sn*-2-acyllysophosphatidic acid resulting from the neutral loss of vinylamine. Less abundant product ions including *m*/*z* 441 ($[M + Na - 61]^+$) result from the neutral loss of ethanolamine resulting in the generation of a sodiated monoacyl glycerophosphodiester. The neutral loss of sodium ethanolamine phosphate results in the generation of a monoacyl glycerol derivative cation (*m*/*z* 339, $[M + Na - 163]^+$). The structures of these two product ions are completely analogous to product ions corresponding to $[M + Na - 103]^+$ and $[M + Na - 205]^+$ previously identified in tandem mass spectra of sodiated lysophosphatidylcholine (Figures 2 and 3).

The positive-ion ESI tandem mass spectra of *sn*-1 and *sn*-2 regioisomers of sodiated lysophosphatidylethanolamine are dramatically different (compare Figure 6A to Figure 6B). For example, in addition to three informative product ions (*m*/*z* 459, 441, and 339) after dissociation of sodiated *sn*-1-lysophosphatidylethanolamine, three other product ions *m*/*z* 361, 164, and 121 corresponding to a sodiated monoacyl glycerol derivative, sodiated phosphoethanolamine, and sodiated phosphatidic acid, respectively, are present in the positive-ion ESI tandem mass spectrum of sodiated *sn*-2-lysophosphatidylethanolamine (Figure 6B). Furthermore, the product ion pair at *m*/*z* 164 (corresponding to sodiated phosphoethanoalmine) and 441 (corresponding to sodiated monoacyl glycerophosphodiester, i.e., $[M + Na - 61]^+$) demonstrated at 25-fold difference in their ratio in each lysophosphatidylethanolamine regioisomer (i.e., a ratio of approximately 1:10 for *sn*-1-acyllysophosphatidylethanolamine and a ratio of approximate 5:2 for *sn*-2-acyllysophosphatidylethanolamine were present) (Figure 6). Distinction between individual lysophosphatidylethanolamine regioisomers can be further substantiated by the 16-fold difference in the ratio of the relative

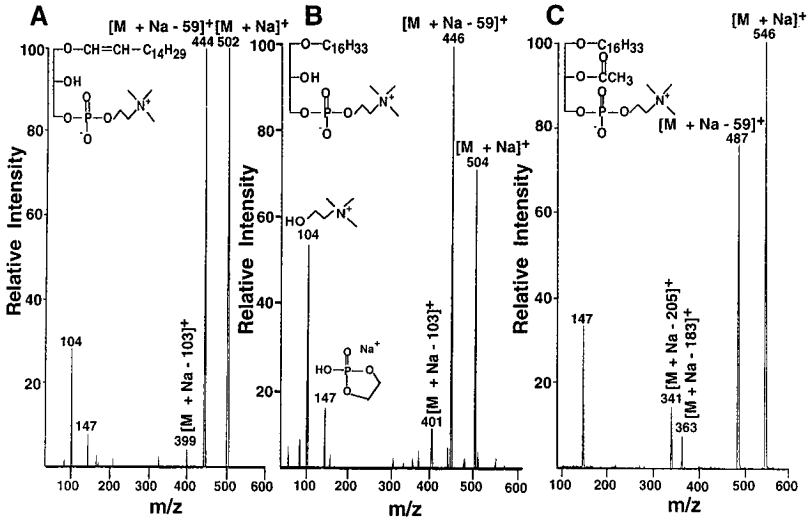

Figure 5. Positive-ion electrospray ionization tandem mass spectrum of lysoplasmenylcholine, lysoplasmanylcholine, and platelet activating factor. Positive-ion ESI tandem mass spectra of sodiated 1-*O-(Z)*-hexadec-1′-enyl-2-hydroxy-*sn*-glycero-3-phosphocholine (i.e., lysoplasmenylcholine) (A), sodiated 1-*O*-hexadecyl-2-hydroxy-*sn*-glycero-3-phosphocholine (i.e., lysoplasmanylcholine) (B), and sodiated 1-*O*-hexadecyl-2-acetyl-*sn*-glycero-3-phosphocholine (i.e., platelet activating factor) (C) were obtained as described in the Experimental Section. Samples (1 pmol/μL) were dissolved in 1:2 chloroform/methanol and infused directly into the ESI chamber using a syringe pump at a flow rate of 1.5 μL/min for 5 min.

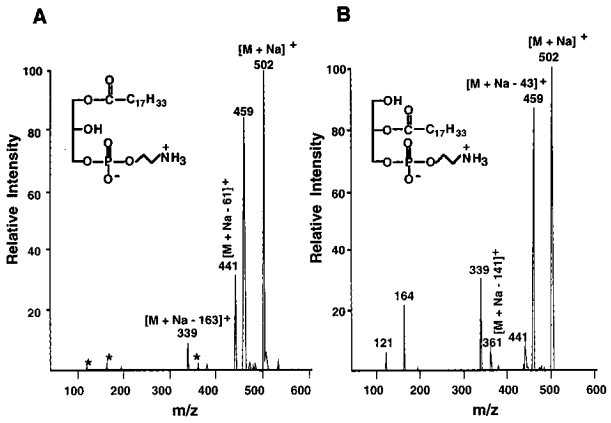

Figure 6. Positive-ion electrospray ionization tandem mass spectra of ethanolamine lysophospholipid regioisomers. Positive-ion ESI tandem mass spectra of sodiated 1-octadec-9′-enoyl-2-hydroxy-*sn*-glycero-3-phosphoethanolamine (A) and sodiated 1-hydroxy-2-octadec-9′-enoyl-*sn*-glycerol-3-phosphoethanolamine (B) were obtained as described in the Experimental Section. Samples (1 pmol/μL) were dissolved in 1:2 chloroform/methanol and infused directly into the ESI chamber at a flow rate of 1.5 μL/min for 5 min. The stars in panel A indicate the presence of product ions at *m*/*z* 121, 164, and 361, present in very low abundance.

intensity of the product ion pair at *m*/*z* 339 ($[M + Na - 163]^+$) and 441 ($[M + Na - 61]^+$) (Figure 6).

Potential Dissociation Pathways of Sodiated Lysophosphatidylethanolamine Regioisomers. Product-ion patterns of sodiated lysophosphatidylethanolamine regioisomers arise from the differences in the relative activation energies (enthalpic and entropic) for collision-induced dissociation of precursor ions (i.e., individual sodiated lysophosphatidylethanolamine regioisomers (Schemes 3 and 4, respectively)). Four main pathways for collision-induced dissociation are likely, including (1) the neutral loss of vinylamine resulting in the generation of sodiated phosphatidic acid (pathway 1); (2) the neutral loss of ethanolamine resulting in the generation of a sodiated 5-membered phosphodiester from sodiated 1-acyl-2-hydroxy-*sn*-glycero-3-phosphoethanolamines (Scheme 3) or a sodiated 6-membered phosphodiester from sodiated 1-hydroxy-2-acyl-*sn*-glycero-3-phosphoethanolamine (Scheme 4) (pathway 2); (3) the neutral loss of sodium ethanolamine phosphate resulting in the generation of a 6-membered oxonium ion from 1-acyllysophosphatidylethanolamine (Scheme 3) or a 5-membered oxonium ion from 2-acyllysophosphatidylethanolamine (Scheme 4) (pathway 3); or (4) a rearrangement resulting in the generation of either a sodiated monoacyl glycerol derivative ($[M + Na - 141]^+$) through the neutral loss of phosphoethanolamine or a sodiated phosphoethanolamine (*m*/*z* 164) through the neutral loss of monoacyl glycerol derivative (pathway 4). Because these pathways emanate from a common molecular ion, the relative abundance of product ions are directly related to the enthalpic and entropic changes between critical intermediates in each pathway. Similar to results deduced from study of the sodiated choline lysophospholipid regioisomers, a 5-membered product ion (in comparison to a 6-membered product ion) is the kinetically favored product in each case. Thus, the favored product of sodiated 1-acyllysophosphatidylethanolamine dissociation corresponds to the sodiated 5-membered phosphodiester ($[M + Na - 61]^+$) while the sodiated 6-membered phosphodiester (formed from sodiated 2-acyllysophosphatidylethanolamines) is present in lower abundance. Similarly, the major product ion ($[M + Na - 163]^+$) from collision-induced dissociation of sodiated 2-acyllysophosphatidylethanolamine

Scheme 3. Proposed Collision-Induced Dissociation Pathways of Sodiated 1-Acyl-2-hydroxy-*sn*-glycero-3-phosphoethanolamines

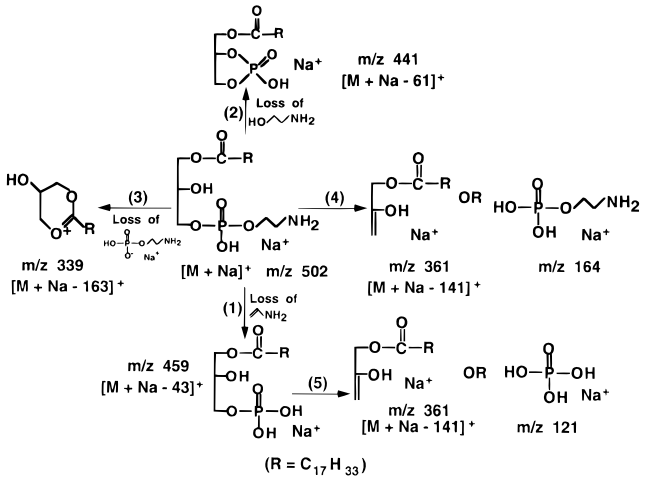

Scheme 4. Proposed Collision-Induced Dissociation Pathways of Sodiated 1-Hydroxy-2-acyl-*sn*-glycero-3-phosphoethanolamines

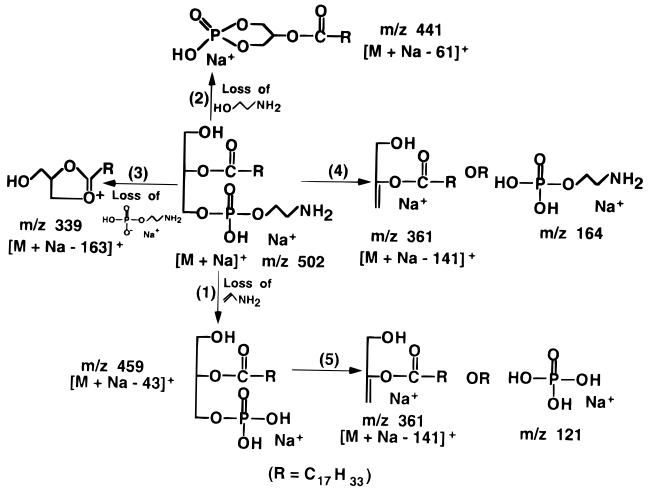

corresponds to the 5-membered oxonium ion while the corresponding 6-membered analog formed from sodiated 1-acyllysophosphatidylethanolamine is present in lower relative abundance. The dissociation pathways 4 and 5 reflect an activated rearrangement (activated by the electron-withdrawing properties of the ester group) in the case of sodiated 2-acyllysophosphatidylethanolamine or a nonactivated rearrangement in the case of sodiated 1-acyllysophosphatidylethanolamine or a nonactivated rearrangement in the case of sodiated 1-acyllysophosphatidylethanolamine. Furthermore, the dissociation pathways 4 and 5 in the case of sodiated 1-acyl-2-hydroxy-*sn*-glycero-3-phosphoethanolamine (Scheme 3) involve the formation of a compound containing a vinyl alcohol which is less stable than the corresponding vinyl ester formed from sodiated 1-hydroxy-2-acyl-*sn*-glycero-3-phosphoethanolamine (Scheme 4). Accordingly, the ion $[M + Na - 141]^+$ and ions at *m*/*z* 164 and 121 are predominant product ions in the case of sodiated 2-acyllysophosphatidylethanolamine but represent only minor constituents in the case of sodiated 1-acyllysophosphatidylethanolamine.

Negative-Ion ESI Tandem Mass Spectrometry of Choline and Ethanolamine Lysophospholipids. Although these studies demonstrate that the regiospecificity of lysophospholipid positional isomers can be identified by positive-ion ESI tandem mass spectrometry, product ions corresponding to the aliphatic chain constituent cannot be individually identified in the positive-ion mode. Accordingly, negative-ion ESI tandem mass spectrometry of lysophospholipids was employed to identify aliphatic chain constituents. Selection and collisional activation of the chlorine adduct $[M + Cl]^-$ (the major quasi molecular ion when chloride is present[26]) of 1-acyl-2-hydroxy-*sn*-glycero-3-phosphocholines after ESI in negative-ion mode resulted in multiple informative product ions. For example, a negative-ion ESI tandem mass spectrum of the chlorine adduct of 1-hexadecanoyl-2-hydroxy-*sn*-glycero-3-phosphocholine demonstrated a predominant product ion at *m*/*z* 480 (i.e., $[M + Cl - CH_3Cl]^-$) corresponding to the neutral loss of CH_3Cl from precursor $[M + Cl]^-$ ion to form a *N*,*N*-dimelthyllysophosphatidylethanolamine anion (Figure 7A). Other less abundant product ions include ions at *m*/*z* 255, 224, and 242 (palmitate, neutral loss of hexadecanoic acid, and neutral loss of hexadecyl ketene from *N*,*N*-dimethyllysophosphatidylethanolamine anion ($[M + Cl - CH_3Cl]^-$), respectively). The negative-ion ESI tandem spectrum of chlorine adduct of 1-hydroxy-2-acyl-*sn*-glycero-3-phosphocholine (spectrum not shown) was nearly identical to that derived

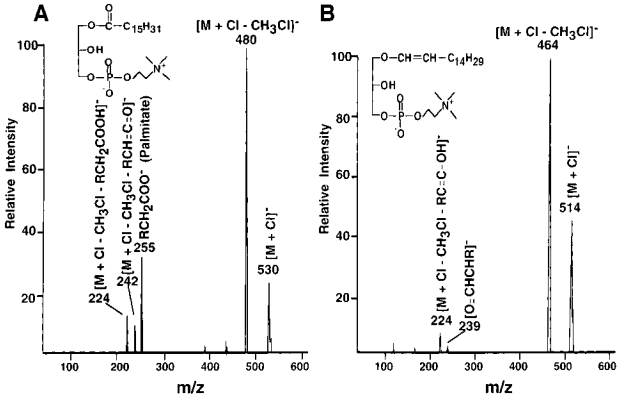

Figure 7. Negative-ion electrospray ionization tandem mass spectra of choline lysophospholipids. (A) Negative-ion ESI tandem mass spectrum of the chlorine adduct of 1-hexadecanoyl-2-hydroxy-*sn*-glycero-3-phosphocholine (palmitoyl lysophosphatidylcholine). (B) Negative-ion ESI tandem mass spectrum of the chlorine adduct of 1-*O*-*(Z)*-hexadec-1′-enyl-2-hydroxy-*sn*-glycero-3-phosphocholine (palmitoyl lysoplasmenylcholine). Each choline lysophospholipid (1 pmol/μL) was dissolved in 1:2 chloroform/methanol with coaddition of NaCl (5 pmol/μL) prior to performance of ESI tandem mass spectrometry in the negative-ion mode as described in the Experimental Section.

from the chlorine adduct of 1-acyl-2-hydroxy-*sn*-glycero-3-phosphocholine. Thus, the regiospecificity of choline lysophospholipids cannot be determined by negative-ion ESI tandem mass spectrometry alone. As anticipated, the carboxylate product ion is absent in the negative-ion ESI tandem mass spectra of the chlorine adduct of lysoplasmenylcholine and lysoplasmanylcholine. For example, the negative-ion ESI tandem mass spectrum of the chlorine adduct of 1-*O*-*(Z)*-hexadec-1′-enyl-2-hydroxy-*sn*-glycero-3-phosphocholine (lysoplasmenylcholine) contains a major product ion at *m*/*z* 464 and two minor product ions at *m*/*z* 239 (palmityl aldehyde anion) and 224 (corresponding to the neutral loss of palmitenyl alcohol) (Figure 7B).

Negative-ion ESI tandem mass spectra of lysophosphatidylethanolamine regioisomers displayed a major product ion, corresponding to the carboxylate ion of the acyl chain (e.g., Figure 8A). Several minor product ions derived from the glycerol backbone and polar head group including ions at *m*/*z* 196, 153, and 140 were present which likely correspond to the loss of H_2O from the glycerophosphoethanolamine anion, the loss of H_2O from glycerol phosphate, and the phosphoethanolamine anion, respectively. These minor product ions were typically not detected under similar conditions in negative-ion tandem mass spectra of phosphatidylethanolamine.[27] As anticipated, the negative-ion ESI tandem mass spectra of lysoplasmenylethanolamine and lysoplasmanylethanolamine differed from those of corresponding lysophosphatidylethanolamine since the major product ion (i.e., the carboxylate ion) was absent and was replaced by a low-abundance product ion corresponding to the *sn*-1-alkenyl or -alkyl chain (verified by varying the chain length of lysoplasmenylethanolamines shown in Figures 8B and 8C). An additional product ion (i.e., $[M - 62]^-$, corresponding to the neutral loss of ethanolamine from precursor ion) was present in the negative-ion ESI tandem mass spectra of lysoplasmenylethanolamine and lysoplasmanylethanolamine. The product ion at *m*/*z* 196 (corresponding to the loss of H_2O from glycerol phosphoethanolamine) was the most abundant product ion under the experimental conditions employed. These differences in observed product ion intensities are due to the relatively higher stability of the *sn*-1 ether linkage in lysoplasmenylethanolamine and lysoplasmanylethanolamine in comparison to the ester linkage in lysophosphatidylethanolamine.

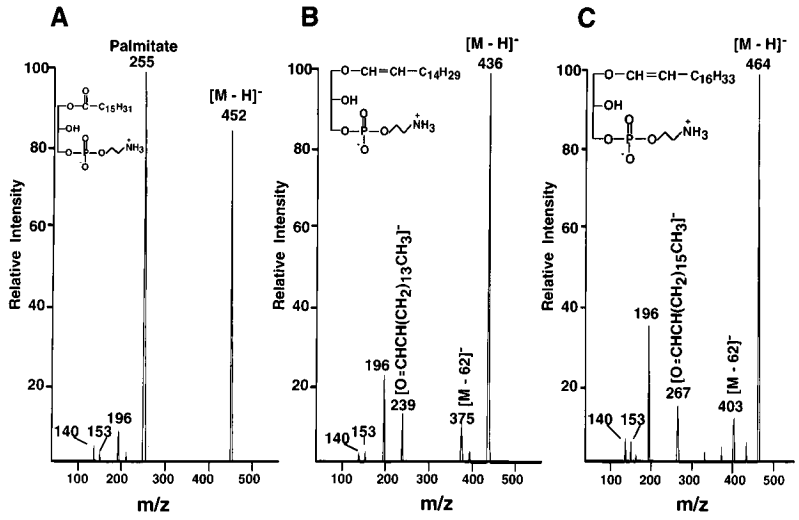

Figure 8. Negative-ion electrospray ionization tandem mass spectra of ethanolamine lysophospholipids. (A) Negative-ion ESI tandem mass spectrum of 1-hexadecanoyl-2-hydroxy-*sn*-glycero-3-phosphoethanolamine (palmitoyllysophosphatidylethanolamine). (B) Negative-ion ESI tandem mass spectrum of 1-*O-(Z)*-hexadec-1′-enyl-2-hydroxy-*sn*-glycero-3-phosphoethanolamine (palmitoyllysoplasmenylethanolamine). (C) Negative-ion ESI tandem mass spectrum of 1-*O-(Z)*-octadec-1′-enyl-2-hydroxy-*sn*-glycero-3-phosphoethanolamine (stearoyllysoplasmenylethanolamine). Each ethanolamine lysoglycerophospholipid (1 pmol/μL) was dissolved in 1:2 chloroform/methanol prior to performance of ESI tandem mass spectrometry in negative-ion mode as described in the Experimental Section.

Conclusion

The results presented herein demonstrate the remarkable capability of the combined utilization of positive- and negative-ion ESI tandem mass spectrometry for the direct structural determination of lysophospholipid regioisomers, classes, subclasses, and individual molecular species from picomole amounts of material. Through exploiting differences in the intensity of diagnostic pairs of product ions produced during collisional activation, well-defined kinetic determinants dictate the relative flux of precursor ion into competing dissociation pathways, thereby facilitating the discrimination of lysophospholipid regioisomers.

Acknowledgment. This research was supported by NIH Grant HL#41250 and the Washington University Mass Spectrometry Resource NIH Grant RR95418.

JA952326R